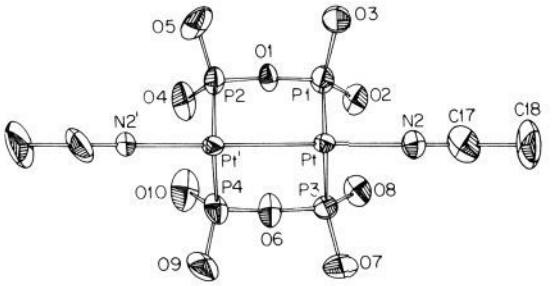

Figure 1. Perspective view of $[Pt_2(P_2O_5H_2)_4(CH_3CN)_2]^{2-}$. For clarity, *only two bridging pyrophosphites are shown. The primed atoms are* related to the unprimed ones by the inversion center at the origin. The thermal ellipsoids are drawn at the 35% probability level.

The structure and atom labeling scheme of the binuclear platinum(III) anion are illustrated in Figure 1.[7] The complex consists of two face-to-face square-planar PtP_4 units linked by four pyrophosphite groups,[4] with two axial CH_3CN ligands trans to the Pt–Pt bond. The observed Pt–Pt distance of 2.676 (1) Å is shorter than that in any of the structurally characterized $[Pt_2(P_2O_5H_2)_4X_2]^{4-}$ complexes.[4] Comparison of the structures of $[Pt_2(P_2O_5H_2)_4(CH_3CN)_2]^{2-}$ and $[Pt_2(P_2O_5H_2)_4(CH_3)(I)]^{4-}$ (d(Pt–Pt) = 2.782 (1) Å)[4d] reveals that the Pt–Pt bond can be varied over 0.1 Å by axial ligation. The mean Pt–P distance of 2.369 Å and P–O–P angle of 125° are similar to those found for $[Pt_2(P_2O_5H_2)_4Cl_2]^{4-}$[4e] and $[Pt_2(P_2O_5H_2)_4(SCN)_2]^{4-}$.[4b] The Pt–N distance of 2.093 (10) Å is shorter than that found in $[Pt_2(P_2O_5H_2)_4(NO_2)_2]^{4-}$ (2.147 Å)[4b,g] and $[Pt_2(P_2O_5H_2)_4(Im)_2]^{4-}$ (2.13 Å).[4b] Interestingly, the coordinated CH_3CN of $[Pt_2(P_2O_5H_2)_4(CH_3CN)_2]^{2-}$ is not substitutionally labile, as the conversion of $[Pt_2(P_2O_5H_2)_4(CH_3CN)_2]^{2-}$ to $[Pt_2(P_2O_5H_2)_4Cl_2]^{4-}$ in 0.1 M HCl takes more than 1 h.

The UV–vis spectrum of $[Pt_2(P_2O_5H_2)_4(CH_3CN)_2]^{2-}$ in acetonitrile (or water) solution exhibits an intense band centered at 211 nm (ϵ 46 500) (Figure 2). Owing to the high ionization energy of the lone-pair σ(N) orbital of CH_3CN, the highest-occupied σ level of the d^7–d^7 complex should be the bonding combination of $5d_{z^2}$ Pt orbitals. Thus $[Pt_2(P_2O_5H_2)_4(CH_3CN)_2]^{2-}$ contains a relatively localized Pt–Pt($d\sigma^2$) single bond, and the 211-nm band is attributable to the fully allowed $d\sigma \rightarrow d\sigma^*$ transition.[8] The relatively high energy of a (Pt–Pt)-localized $d\sigma \rightarrow d\sigma^*$ excitation clearly shows that the lowest $\sigma \rightarrow d\sigma^*$ systems in $[Pt_2(P_2O_5H_2)_4X_2]^{4-}$ species possess substantial $X \rightarrow Pt$ charge-transfer character and accordingly should be designated as $\sigma(X) \rightarrow d\sigma^*$ transitions. The observed dependence of the transition wavelength on X(Cl (282) < Br (305) < SCN (337) ~ I (338 nm))[4a] strengthens this interpretation. The intense band at ~215 nm

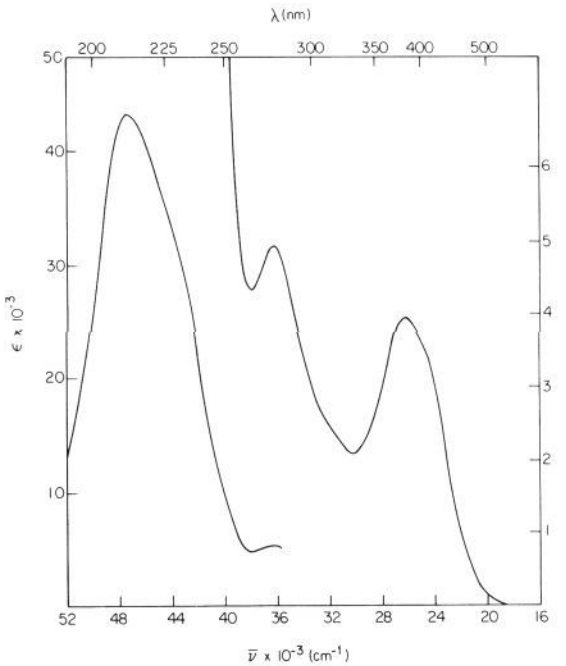

Figure 2. UV–vis absorption spectrum of $[Pt_2(P_2O_5H_2)_4(CH_3CN)_2]^{2-}$ in CH_3CN at room temperature.

(X = Cl, Br, I)[5] is logically the $d\sigma \rightarrow d\sigma^*$ transition in these complexes.

Acknowledgment. This research was supported by the Committee of Conference and Research Grants of the University of Hong Kong and National Science Foundation Grant CHE84-19828.

Supplementary Material Available: Tables of atomic coordinates, thermal parameters and selected bond distances and angles (5 pages). Ordering information is given on any current masthead page.

(7) Crystal data for $[Bu_4N]_2[Pt_2(P_2O_5H_2)_4(CH_3CN)_2]$: space group, $P2_1/n$, a = 11.296 (8) Å, b = 21.199 (5) Å, c = 12.580 (5) Å, β = 92.46 (4)°, z = 2, f (000) = 1532, d_{measd} = 1.695 g cm^{-3}, d_{calcd} = 1.691 g cm^{-3}. A 0.24 × 0.20 × 0.16-mm crystal was used for data collection. Intensities (h, k, $\pm l$; 5288 unique data) were measured at 22 °C on a Nicolet R3m diffractometer using the ω–2θ variable-scan 2.02–8.37 deg min^{-1}) technique in the bisecting mode up to $2\theta_{max}$ = 50°. Azimuthal scans of selected strong reflections over a range of 2θ values were used to define a pseudoellipsoid for the application of absorption corrections (μr = 0.50, transmission factors 0.242–0.288). The structure solution was accomplished by means of Patterson and Fourier methods. The binuclear platinum(III) anion occupies a centrosymmetric site in the crystal lattice. All non-hydrogen atoms in the asymmetric unit were varied anisotropically. For the organic cation, the hydrogen atoms were generated geometrically (C–H fixed at 0.96 Å) and included in structure factor calculations with assigned isotropic thermal parameters; the methyl hydrogen atoms were allowed to ride on their respective parent carbon atoms, and the methyl groups were treated as rigid groups. Blocked cascade least-squares refinement converged to R_F = 0.055, R_G = 0.063, and S = 1.177, where $R_F = \sum||F_o| - |F_c||/\sum|F_o|$, $R_G = [\sum w(|F_o| - |F_c|)^2/\sum w|F_o|^2]^{1/2}$ ($w = [\sigma^2(F_o) + 0.0012|F_o|^2]^{-1}$), and $S = [\sum w||F_o| - F_c|)^2(n - p)]^{1/2}$ (n = 3713, number of observed data with $|F_o| > 3\sigma(|F_o|)$, and p = 328, number of variables).

(8) The weaker absorption bands at 380, 276, and 232 nm (sh) (Figure 2) are similar both in positions and intensities to features observed in the spectra of other axially ligated d^7–d^7 platinum[4a] and rhodium[3] species. The lowest two bands in the spectrum of $[Pt_2(P_2O_5H_2)_4(CH_3CN)_2]^{2-}$ are attributable to $d\pi \rightarrow d\sigma^*$ transitions.[3]

Substrate-Leash Amplification of Ribonuclease Activity

Douglas J. Cecchini, Markus Ehrat,† and Roger W. Giese*

Department of Medicinal Chemistry in the College of Pharmacy and Allied Health Professions and Barnett Institute of Chemical Analysis and Materials Science, Northeastern University Boston, Massachusetts 02115

Received May 6, 1986

Chemical amplification takes place when a limited chemical stimulus triggers an enhanced chemical response, as has been reviewed.[1] Here we present a new concept for such amplification, shown in Figure 1. The key feature is that the inactive S-peptide and S-protein fragments of ribonuclease A[2] (RNase) are immobilized on separate chromatographic gels via a polycytidylic acid (poly C) substrate leash. The addition of free RNase initiates cleavage of this leash. When released S-peptide recombines with the immobilized S-protein, active RNase S forms. The RNase S in turn releases additional enzyme, giving a cascade of enzymatic activity.

† Present address: Ciba-Geigy, Basel, Switzerland.

(1) Blaedel, W. J.; Boguslaski, R. C. *Anal. Chem.* **1978**, *50*, 1026–1032.
(2) Richards, F. M.; Wyckoff, H. W. In *The Enzymes*; Boyer, P. D., Ed.; Academic Press: New York, 1971; Vol. IV, pp 647–806.

0002-7863/86/1508-7841$01.50/0

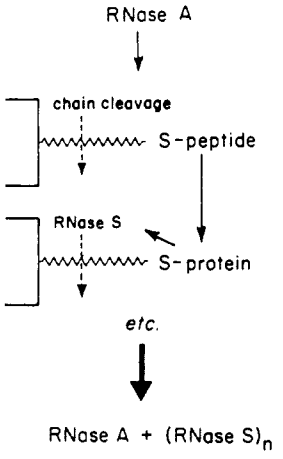

Figure 1. Concept for substrate-leash amplification of ribonuclease activity.

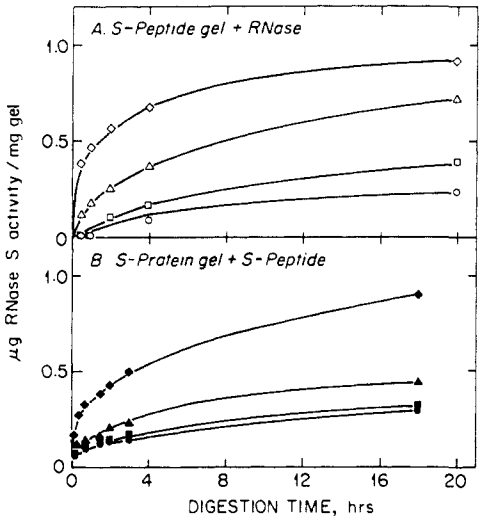

Figure 2. (A) Release of immobilized S-peptide from poly-C-Thiol-Sepharose 4B in 0.0 (○), 0.07 (□), 0.7 (▲), and 7.0 (◊) nM RNase solution. (b) Release of immobilized S-protein from poly-C-Thiol-Sepharose 4B in 0.0 (●), 0.7 (■), 7.0 (▲), and 70 (♦) nM S-peptide solution. One-milligram portions of each gel were separately suspended in 1 mL of 0.5 M Tris, 5 mM EDTA, 0.1% BSA buffer, pH 7.5. RNase or S-peptide was added in 40 μL of buffer giving the final concentrations cited above. The tubes were incubated at room temperature with gentle rocking. Intermittently the suspensions were centrifuged and 25-μL aliquots of the supernatants were added to an excess of the complementary RNase S fragment and assayed for RNase activity. For the S-peptide gel, the contribution of added RNase A activity was subtracted out.

N^4-(Diaminooctyl)polycytidylic acid[3] (DAO-poly C) was selected as the substrate leash. The DAO-poly C was reacted with an excess of N-[(γ-maleimidobutyryl)oxy]succinimide, yielding MI-DAO-poly C. S-Peptide was labeled with N-succinimidyl-3-(2-pyridyldithio)propionate (SPDP), reduced with ethanethiol, and reacted with an excess of MI-DAO-poly C. Taking advantage of the excess MI groups, the resulting conjugate was immobilized onto Thiol-Sepharose 4B or Thiopropyl Sepharose 6B (Pharmacia). In a typical gel we found 23 μg of poly C and 7.3 μg of S-peptide per mg of vacuum-dried gel. Similarly the S-protein of RNase was immobilized via poly C onto Thiol-Sepharose 4B, giving 60 μg of DAO-poly C and 23.8 μg of S-protein per mg of gel. Synthetic and characterization details of these two gels are presented elsewhere.[4]

When the S-peptide gel was treated with RNase, release of S-peptide into the supernatant was observed (Figure 2A). The rate of release was dependent on the dose of RNase. Comparable results were obtained when the S-peptide gel was incubated with S-protein instead of RNase (data not shown). Similarly, the dose-dependent release of substrate-immobilized S-protein following the addition of S-peptide is shown in Figure 2B. Liberation of the S-protein from the gel was also observed when RNase was used in place of the S-peptide (data not shown). Background activity (Figure 2A,B, zero dose) was present in both cases.[5]

Table I. Multistage Amplification of Ribonuclease Activity

stage	eluted RNase S, ng[a] dose RNase A: 0 ng	1 ng	amp factor[b] (cummulative)
1	0	4.9	4.9×
2	31	83	52×
3	100	125	25×

[a] All tubes were done in duplicate, and the values were within ±9% of the average values shown. RNase activity is expressed relative to a standard curve prepared with RNase A. [b] An example calculation for the amplification factor: 52 = (83 − 31) ÷ 1.

Initially we demonstrated the catalytic amplification of RNase using the S-peptide gel alone. A 100-pg dose of RNase was incubated for 20 h with a 50-μL slurry containing 2 mg of this gel. One milliliter of buffer was added and the supernatant was separated by centrifugation and combined with excess S-protein, and RNase S activity was determined. The gels that were treated with 100 pg of RNase yielded an average of 2.77 μg of RNase S activity. After subtraction of the background activity (0.87 μg) obtained in a parallel experiment without the addition of RNase, this corresponds to a 1.9×10^4 amplification of the signal for the initial 100-pg dose.

Encouraged by this result, we proceeded to demonstrate multistage amplification of RNase activity. One nanogram of RNase was passed through a three-stage system in 150 μL of pH 5 acetate buffer. Each stage consisted of an incubation with 2 mg of S-peptide gel followed by an incubation with 2 mg of the S-protein gel. The incubation time was 30 min for the first S-peptide gel and 15 min for each of the subsequent gels. The solution was transferred from one gel to the next by centrifugation through a filter. RNase S activity was measured after each stage, giving the results shown in Table I. The amount of amplification was calculated relative to the initial 1-ng dose of RNase after correcting for the background activity obtained from a 0 dose. The maximum total amplification was achieved (52 times the initial amount of RNase) after the second stage. The overall degree of amplification decreased in stage 3, largely due to the increase in background activity.[5] While a constant multiplication factor is anticipated, we found a 4.9-fold increase in RNase activity in stage 1 and a 10.6-fold increase in stage 2. This could be rationalized as a dilution effect since the increasing concentration of the RNase S components with time would favor their recombination to form active RNase S, causing a more rapid digestion of the gel.[6]

The turnover number of RNase toward cytidyl-(3′→5′)-cytidine is 160 s^{-1} at 25 °C.[2] If conditions could be established for generating RNase S in a substrate-leash device at an overall rate corresponding to 0.001 of this V_{max} (an arbitrary but reasonable reference point), then the degree of amplification after 2 min would be 6×10^5, after 3 min 4.7×10^8, etc. Thus, the initial amplification reported here is only a small fraction of that potentially available with this approach.

The concept of substrate-leash amplification can be broadened to comprise other molecular chain and release components besides

(3) Ehrat, M.; Cecchini, D. J.; Giese, R. W. *J. Chromatogr.* **1985**, *326*, 311–320.
(4) Ehrat, M.; Cecchini, D. J.; Giese, R. W. *Clin. Chem.*, in press.

(5) Residual contaminating RNase activity associated with the RNase fragments, particularly with the S-protein which possessed 0.02% activity, no doubt contributes to the spontaneous release of the immobilized fragments. Improved performance of our system is anticipated once these components are further purified.
(6) Consistent with the known affinity constant of 7×10^9 M^{-1} for the association of S-peptide with S-protein (Blackburn, P.; Moore, S. In *The Enzymes*; Boyer, P. D., Ed.; Academic Press: New York, 1982; Vol. 15, pp 319–434), we have observed that the specific activity of RNase S, native or assembled from our modified fragments, decreases with increasing dilution.

those presented here. Other surfaces such as membranes can be explored. Applications to assays that involve enzyme labels (e.g., immunoassays and DNA probe assays) and to biosensors are anticipated.

Acknowledgment. This work was supported by DARPA Contract N00014-84-C-0254 administered by the Office of Naval Research. Contribution No. 276 from the Barnett Institute of Chemical Analysis. In memory of Wallace A. Giese.

Registry No. RNaseA, 9001-99-4.

Interligand and Charge-Transfer Emission from $[Ru(bpy)(HDPA)_2]^{2+}$: A Dual Emitting Ru(II) Complex

Richard L. Blakley, Michael L. Myrick, and M. Keith DeArmond*

Department of Chemistry, North Carolina State University Raleigh, North Carolina 27695-8204

Received June 9, 1986

Tris-chelated complexes with bidentate α,α'-diimine ligands such as bipyridine and phenanthroline have been shown to have single ligand localized emitting states.[1,2] Therefore, in mixed-ligand complexes a dual emission might be expected since localized states involving each type of ligand would exist. Such a result occurs for the $[Rh(bpy)_n(phen)_{3-n}]^{2+}$ (n = 1, 2) complexes where a $\pi-\pi^*$ emission is observed from both a coordinated bpy and a coordinated phen.[3] This type of mulitple luminescence is termed "spatially isolated" since the emissions are from spatially distinct regions of the molecule.[4] A second type of dual emission is found for $[Ir(phen)_2Cl_2]^+$ where both a d–d* and a d–π^* emission occur.[5] Since these emitting states have different orbital origins, this type of phenomena is termed "distinct orbital".[4] Even though photoselection data for $[Ru(bpy)_3]^{2+}$ indicates a single ligand emission,[1,2] no dual luminescence could be characterized for the $[Ru(bpy)_n(phen)_{3-n}]^{2+}$ (n = 1, 2) ions[6] due to the fact that the MLCT emissions from the two chromophores have virtually identical energies, contours, and lifetimes, thus precluding energy or time resolution. Other Ru(II) mixed-ligand complexes[7,8] obey Kasha's rule[4] with relaxation occurring from the higher energy chromophore to the lower energy radiative chromophore. In Ru(II) complexes involving the nonplanar ligand HDPA (2,2′-dipyridylamine) which has an amine function ~0.2 nm from the π system of an adjacent ligand,[9] the electrochemistry[10] is different from $[Ru(bpy)_3]^{2+}$, the former species being easier to oxidize but more difficult to reduce. Spectroscopy of Ru complexes with an HDPA ligand[11] has shown an emission close in energy to the emission observed for $[Ru(bpy)_3]^{2+}$, inferring mixed-ligand complexes of HDPA and bpy might have a detectable dual luminescence. We now wish to report the first dual emission for a Ru(II) complex, since to date no bona fide Ru(II) dual emission has been reported.[12-14]

Table I. Low-Temperature (77 K) Lifetimes Measured at the Emission Maxima

complex	solvent	$\bar{\nu}$, cm^{-1}	77 K, us[a]
$[Ru(bpy)(HDPA)_2]^{2+}$	H_2O	14 800	2.54 ± 0.09
	ETOH	16 400	13.3 ± 0.5
	ETOH	14 900	5.04 ± 0.3
$[Ru(bpy)_2(HDPA)]^{2+}$	H_2O	15 500	2.91 ± 0.08
	ETOH	16 400	4.60 ± 0.11
$[Ru(bpy)_3]^{2+}$	H_2O	16 900	3.67 ± 0.14
	ETOH	17 300	5.94 ± 0.29

[a] Errors are the calculated 95% confidence limits.

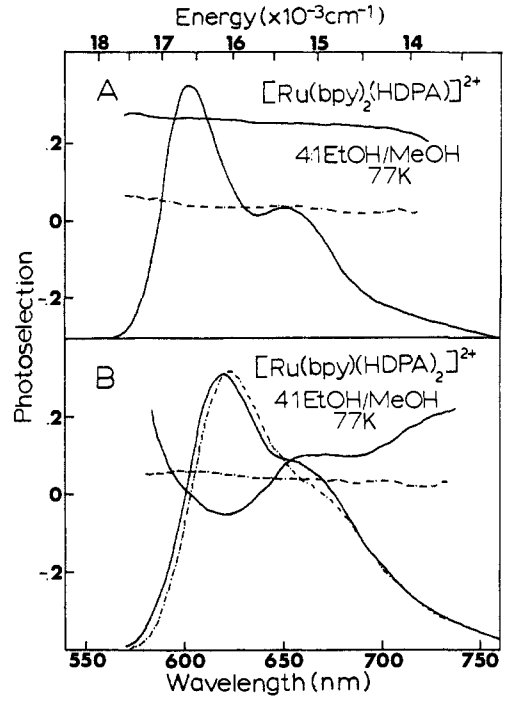

Figure 1. Emission photoselection (77 K) (350 (---) and 460 nm (—) excitation) plotted across the 77 K emission spectrum in 4:1 EtOH/MeOH for (A) $[Ru(bpy)_2(HDPA)]^{2+}$ and (B) $[Ru(bpy)(HDPA)_2]^{2+}$.

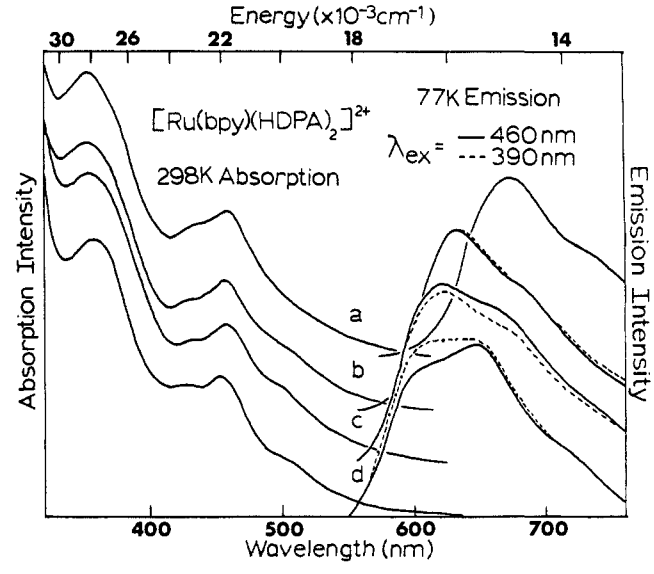

Figure 2. Room temperature absorption and the 77 K emission spectra (460 and 390 nm excitation) for $[Ru(bpy)(HDPA)_2]^{2+}$ in the solvents (a) H_2O, (b) MeOH, (c) EtOH, and (d) 2-PrOH. The intensity scales are offset for clarity.

(1) Carlin, C. M.; DeArmond, M. K. *Chem. Phys. Lett.* **1982**, *89*, 297.
(2) Carlin, C. M.; DeArmond, M. K. *J. Am. Chem. Soc.* **1985**, *107*, 53.
(3) Halper, W.; DeArmond, M. K. *J. Lumin.* **1972**, *5*, 225.
(4) DeArmond, M. K.; Carlin, C. M. *Coord. Chem. Rev.* **1981**, *36*, 325.
(5) Watts, R. J.; Brown, M. J.; Griffith, B. G. *J. Am. Chem. Soc.* **1975**, *97*, 6029.
(6) Crosby, G. A.; Elfring, W. H., Jr. *J. Phys. Chem.* **1976**, *80*, 2206.
(7) Juris, A.; Barigelletti, F.; Balzani, V.; Belsar, P.; Von Zelewsky, A. *Inorg. Chem.* **1985**, *24*, 202.
(8) Barigelletti, F.; Belser, P.; Von Zelewsky, A.; Juris, A.; Balzani, V. *J. Phys. Chem.* **1985**, *89*, 3680.
(9) This value is estimated from molecular models since X-ray results are not available for the mixed-ligand complexes.
(10) Morris, D. E.; Ohsawa, Y.; Segers, D. P.; DeArmond, M. K.; Hanck, K. W. *Inorg. Chem.* **1984**, *23*, 3010.
(11) Segers, D. P.; DeArmond, M. K. *J. Phys. Chem.* **1982**, *86*, 3768.

0002-7863/86/1508-7843$01.50/0